MICROSTRUCTURAL EVOLUTION IN A NI- BASED SUPERALLOY FOR POWER PLANT APPLICATIONS AS A CONSEQUENCE OF High TEMPERATURE DEGRADATION AND REJUVENATION HEAT TREATMENTS

Z. Yao[1], M. A. E. Jepson[1] and R. C. Thomson[1]
[1]Department of Materials, Loughborough University, Loughborough, LE11 3TU, UK
C. C. Degnan[2]
[2]E.ON New Build & Technology Limited, Technology Centre, Ratcliffe-on-Soar, Nottingham, NG11 0EE, UK

ABSTRACT

The microstructural evolution of the Ni-based superalloy CMSX-4 including the change in gamma prime size and distribution and the degree of rafting has been examined in detail using field emission gun scanning electron microscopy (FEGSEM) and transmission electron microscopy (TEM) after high temperature degradation and rejuvenation heat treatments. The relationship between the microstructure, mechanical properties and the applied heat treatment procedures has been investigated. It is shown that there are significant differences in the rafting behaviour, the size of the 'channels' between the gamma prime particles, the degree of rafting and the size of the tertiary gamma prime particles in each of the different microstructural conditions studied. Chemical segregation investigations were carried out to establish the cause of reduced mechanical properties of the rejuvenated sample after high temperature degradation compared to an as-received sample after the same degradation procedure. The results indicate that although the microstructure of as-received and rejuvenated samples were similar, the chemical segregation was more pronounced in the rejuvenated samples, suggesting that chemical segregation from partitioning of the elements during rejuvenation was not completely eliminated. The aim of this research is to provide greater understanding of the suitability of rejuvenation heat treatments and their role in the extension of component life in power plant applications.

INTRODUCTION

Ni-based superalloys are widely used in power generation as gas turbine components due to their excellent high temperature performance. These components are subjected to a combination of elevated temperature, high stress and aggressive environments during service, which inevitably cause various microstructural changes in the material [1-2]. This microstructural deterioration can lead to a degradation of mechanical properties such as tensile strength and creep resistance, which can lead to failure in the components and reduce their service life [3-5]. When a superalloy gas turbine component reaches the end of its predicted life, the user typically has two options: replace the component or attempt to extend its life. Replacement not only requires expensive materials but also adds to the maintenance and operational costs of the turbine, which has made the life extension of components a financially viable alternative. Rejuvenation is designed and used to recover some extra life for expensive Ni-based components by restoring the pre-service microstructure (and, hence mechanical properties) ready for the component's extended life. In the case of the CMSX-4 used for power plant applications, the predicted lifetime is primarily governed by the degradation of the microstructure through the rafting of γ' particles. Therefore, understanding the changes in the size, morphology and distribution of γ' particles before and after high temperature degradation and rejuvenation heat treatments becomes very important. However,

at present, limited information is available about the effect that these types of heat treatment have on the integrity of components. In the absence of mechanical loads, the rafting behaviour of γ′ is associated with the dendritic structure of the alloy, which is governed by the local chemical inhomogeneity or chemical segregation [5]. Hence, it is also important to understanding the effects of chemical segregation on the microstructure of the alloy and its mechanical behaviour [6]. In addition, it is essential to evaluate the refurbishment process though the examination of the microstructure, chemical homogeneity and mechanical performance after application of rejuvenation heat treatments and subsequent microstructural degradation.

EXPERIMENTAL PROCEDURE

CMSX-4 single crystal tensile specimens were supplied by E.ON New Build & Technology Limited which, in order to minimise the effects of misorientation had axes within 7 degrees of <001>. The crystal orientations were determined by the Laue back reflection technique. The nominal chemical composition of the CMSX-4 alloy used in the investigation is given in Table 1.

Table 1: The nominal chemical composition for CMSX-4 used in this study / wt%

Al	C	Co	Cr	Fe	Mo	Nb	Re	Hf	Ta	Ti	W	Ni
5.70	0.0022	9.60	6.28	0.06	0.60	0.01	2.95	0.09	6.49	1.00	6.43	Balance

A heat treatment programme was carried out to enable systematic analysis of the microstructural evolution of the CMSX-4 samples, in comparison with the results obtained from mechanical testing. Details of the precise rejuvenation treatment used is proprietary to E.ON New Build & Technology Limited, but an overview of the heat treatment conditions used in this study are shown in Tables 2 and 3.

Table 2: The CMSX-4 samples with their heat treatment conditions

Sample	Heat Treatments
S 1	As-Received
S 2	Rafted
S 3	Rafted + Rejuvenation 1
S 4	Rafted + Rejuvenation 1 + Rafted
S 5	Rafted + Rejuvenation 2

Tensile testing was performed in accordance with ASTM E8/E8M [7] on a servo-mechanical test frame at room temperature using a stain rate of 0.7 mm min^{-1}. The specimens used were 62 mm long and 10 mm in diameter as shown in Fig. 1. Mechanical test results are available from S1 to S4. Mechanical tests for S5, are ongoing and will be reported later but the microstructural analysis and homogeneity results for all the samples are presented in this paper.

For SEM imaging, specimens were cut and mounted in electrically conductive Bakelite, mechanically polished and then electrolytically etched using 10% orthophosphoric acid in water at a voltage of 10 V. The majority of the microstructural examination was then carried out using a Carl Zeiss 1530VP FEGSEM, operated at voltages of 10-20 kV and at working distances of 3 and

15 mm when using Inlens and Everhart Thornley secondary electron detectors respectively. A number of magnifications were used to obtain details of the size of the secondary and tertiary γ′ precipitates and the γ channel widths. For chemical segregation analysis, the chemical composition difference between dendrite cores and interdendritic regions of all heat treated samples was obtained using quantitative energy dispersive x-ray spectroscopy (EDS) area analysis by an Oxford Instruments X-max 80 Silicon Drift Detector attached to the FEGSEM. The dendrite structures were marked by hardness indents on etched samples. In order to avoid the influence of etching on the chemical analysis, these etching effects were subsequently removed by polishing. An area measuring 20x20 μm was analysed both within the dendrite cores and interdendritic regions as shown in Fig. 2. The chemical composition difference between the dendrite cores and interdendritic regions was used to represent the chemical segregation within the samples.

Table 3: The details of heat treatments applied to CMSX-4 samples

<table>
<tr><th>Rafted</th><th>Rejuvenation 1</th><th>Rejuvenation 2</th></tr>
<tr><td rowspan="4">Holding at 1050°C for 1000 h</td><td>Solution</td><td>Solution</td></tr>
<tr><td>High temperature solution heat treatment for rejuvenation</td><td>Extended high temperature solution heat treatment for rejuvenation</td></tr>
<tr><td>Ageing</td><td>Ageing</td></tr>
<tr><td>Two step ageing with different temperature holds</td><td>Two step ageing with different temperature holds</td></tr>
</table>

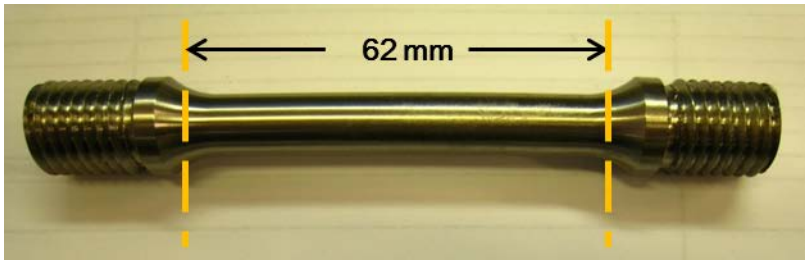

Figure 1: CMSX-4 tensile specimen used in the study.

After the FEGSEM images were taken, further microstructural quantification such as the area fraction of secondary γ′ precipitate particles and γ channel widths were determined using image analysis tools. For the area fraction measurement, suitable contrast and brightness settings were applied to distinguish the secondary γ′ and γ channels to enable thresholding to discriminate the different areas of the microstructure through the use of the image processing software, Image J. For the measurement of the γ channel widths, a grid was placed on the top of the 20,000X magnification images such that the direction of the grid was parallel to the direction of the rafts, as shown in Fig. 3. The channel widths of all channels intercepting each line of the grid were measured manually. Both the channel widths of the parallel and perpendicular direction of the rafts were measured [8]. In order to define the degree of rafting, a rafting parameter introduced by Ignat *et al* [9] was used in this work. The rafting parameter, R, is defined as $R=2L^2/(4LT) = L/(2T)$, where L is the length of rafts and T is the thickness of rafts.

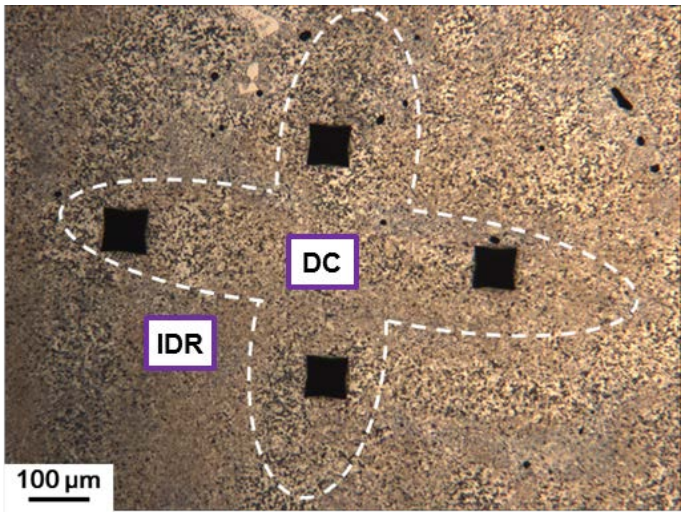

Figure 2: A schematic illustration of the location of the EDS area analysis in the dendritic core (DC) and interdendritic region (IDR) with respect to the dendrite structure.

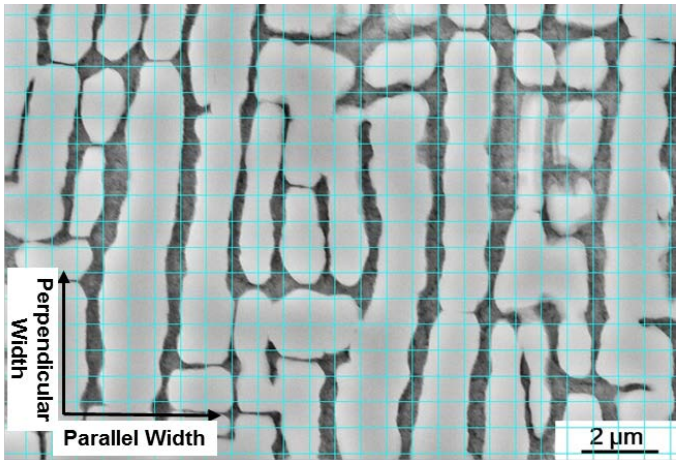

Figure 3: A schematic illustration of the orientation of the perpendicular and parallel channel widths for the measurement of the γ channels for Sample 4.

RESULTS AND DISCUSSION

Tensile Test Data

The tensile curves and results obtained from S1-S4 are shown in Fig. 4 and Table 4. S1 and S3 (as-received and rejuvenation 1) performed similarly in the tensile test but S3 showed a reduced ductility when compared to S1. S1 demonstrated an UTS of 921 MPa and a yield strength of 874 MPa, whilst encouragingly, the measured values of the UTS and yield strength of the rejuvenation 1 sample (S3) were slightly higher at 900 and 900 MPa respectively. The samples after high temperature degradation (S2 and S4) exhibited considerably lower yield strength and UTS, but demonstrated increased levels of ductility.

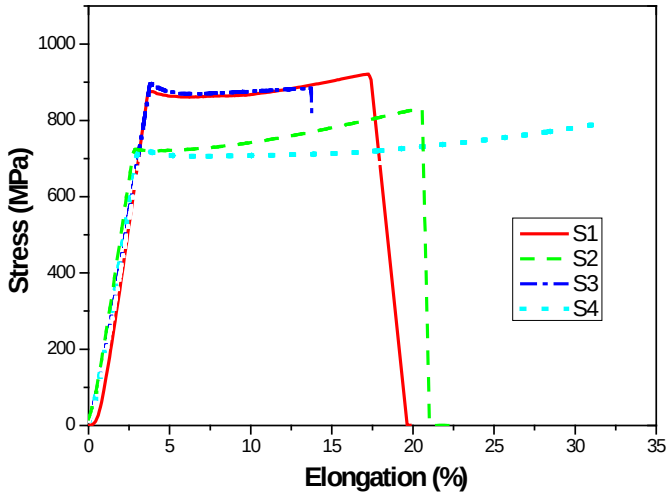

Figure 4: Tensile test results of the four different heat treated conditions for the CMSX-4 samples used in this study.

Table 4: Tensile test results for the four different heat treated samples

Sample No.	Heat Treatments	Yield Strength (MPa)	UTS (MPa)	Elongation (%)
S 1	As-Received	874	921	19.6
S 2	Rafted	724	832	22.7
S 3	Rafted + Rejuvenation 1	900	900	13.7
S 4	Rafted + Rejuvenation 1 + Rafted	728	792	31.9

Microstructural Examination

Figure 5 shows the microstructure of the head sections of the CMSX-4 superalloy samples after five different heat treatments and therefore the microstructures are representative of isothermal ageing only, rather than the application of external load. S1, S3 and S5 exhibited a uniform distribution of the secondary (cuboidal) γ′. S2 and S4 had a rafted microstructure with γ′ particles which have increased in size when compared with the as-received (S1) and rejuvenated samples (S3 and S5) respectively. Tertiary γ′ precipitates in the γ channels between the large γ′ particles were found in all samples except S1. Both very large (>100 nm) and fine (<20 nm) tertiary γ′ particles were found in S2.

TEM was used to further examine the presence of the tertiary γ′ particles and their effects on dislocations within the alloy. The TEM images of the CMSX-4 samples after the five different heat treatments were consistent with the FEGSEM investigations. Tertiary γ′ particles were found in samples S2, S3, S4 and S5, which can act as barriers to block the movement of dislocations. For S2, which has undergone a single rafting process, the tertiary γ′ particles are relatively large at ~100-200 nm, whereas those formed in S4 are considerably smaller (~20 nm) as shown in fig. 6. Dislocations were also observed in S2 and S4, where they were mainly present in the γ channels, especially near the edge of the secondary γ′ particles. These results are consistent with earlier research [11-14].

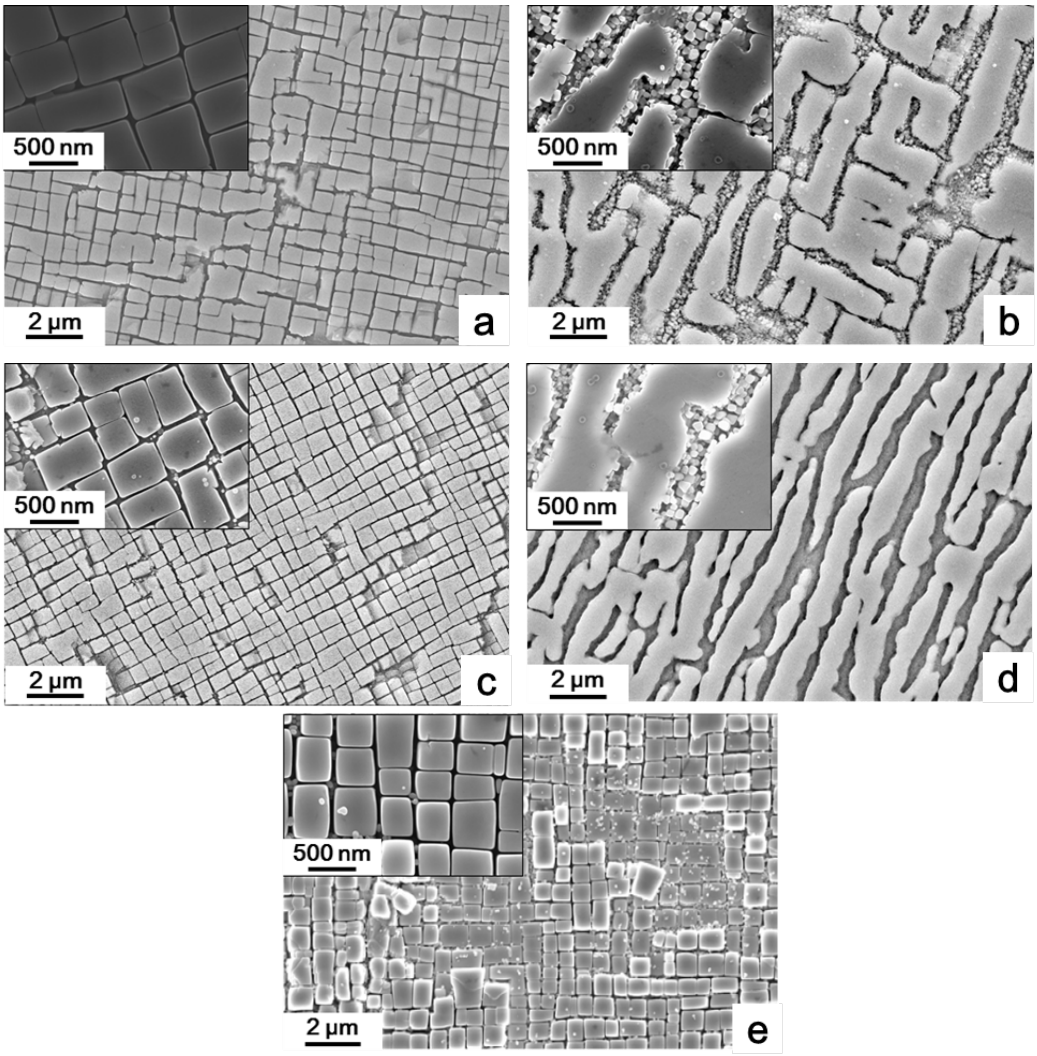

Figure 5: SEM images of the head sections of the CMSX-4 samples after five different heat treatment conditions; a) S1, as-received, b) S2, rafted, c) S3, rafted + rejuvenation 1, and d) S4, rafted + rejuvenation 1+ rafted, e) S5, rafted + rejuvenation 2.

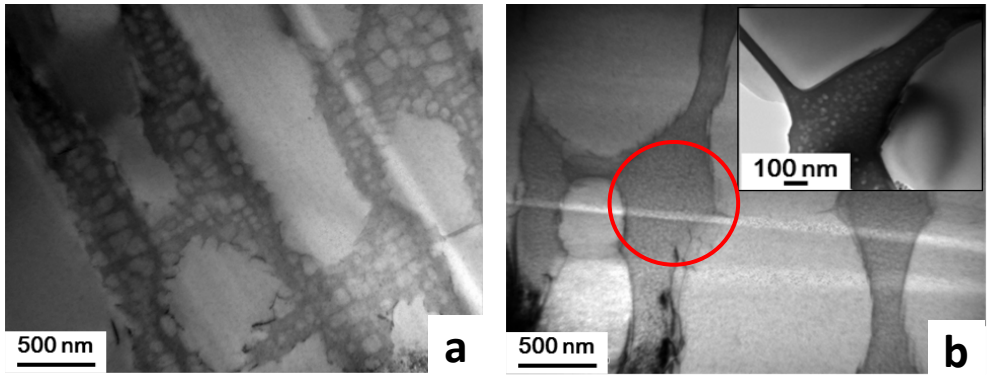

Figure 6: TEM images of the head sections of a) S2, rafted and b) S4, rafted + rejuvenation 1+ rafted with, inset, a high magnification image of the γ channels with tertiary γ′.

Quantification of the γ′ particle sizes and γ channel widths

In order to quantify the microstructural evolution of the CMSX-4 after the different heat treatments, image analysis was carried out to quantify the area fraction of the secondary γ′, γ channel widths and degree of rafting. Figure 7 illustrates the overall results of the area fraction of the secondary γ′ for the head sections of the samples, followed by the channel width measurements and rafting parameter, shown in Table 5 and Fig. 8.

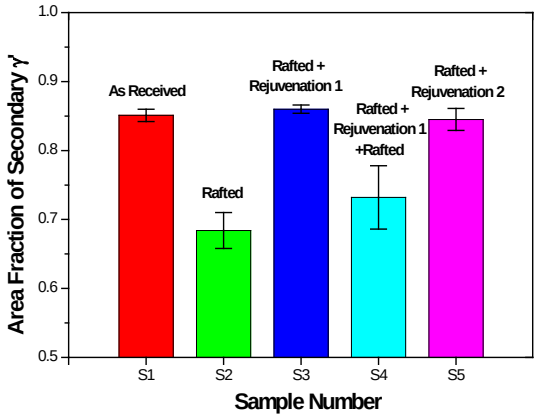

Figure 7: The area fractions of the secondary γ′ particles from the five different heat treatment conditions for the head sections of the tensile test specimens measured using image analysis.

In single crystal Ni-based superalloys, the high level of rupture strength and creep resistance results from the high volume fraction of γ′ contained within the alloy [10]. In this study, the area fraction of the γ′ has been used as an approximation of volume fraction. According to both the tensile test results and the area fraction measurements, the yield and ultimate tensile strength increases with the area fraction of secondary γ′ particles. Although the rafted sample (S2) has the lowest area fraction of secondary γ′ particles, 0.684, it should be noted that there are a large number of tertiary γ′ precipitates in the channels. Moreover, the size of these precipitates is quite large (100-200 nm). The presence of these large tertiary γ′ precipitates in the channels will affect the movement of dislocations, which increases the yield and ultimate strength but reduces the ductility [11-14].

Table 5: The γ channel widths and rafting parameter for the five different heat treated samples

Sample No	Heat Treatments	γ Channel Width / nm		Rafting Parameter
		Parallel	Perpendicular	
S 1	As-received	43±13	39±11	0.56
S 2	Rafted	280±53	250±42	1.64
S 3	Rafted + Rejuvenation 1	58±19	54±17	0.55
S 4	Rafted + Rejuvenation 1 + Rafted	242±81	99±31	2.65
S 5	Rafted + Rejuvenation 2	60±12	59±13	0.53

In order to quantify any influence of the γ channel widths on mechanical properties, these were measured in both the perpendicular and parallel directions with respect to the <001> orientation and are given in Table 5 and Fig. 8. The γ channel widths in the as-received (S1), rejuvenation 1

(S3) and rejuvenation 2 (S5) samples are very small, ~60 nm, whilst those in the degraded structures are much larger, ~300 nm. The small channels of S1 and S3 lead to higher yield and ultimate strengths in the tensile test. The UTS of these samples may be influenced by the movement of dislocations which is governed by the spacing of the γ channels [14]. When the spacing is small, the dislocation has to move through the precipitates by shearing or cutting. The dislocation movement is thus impeded, leading to an increase in the applied stress and hence higher mechanical properties. When the spacing is larger, as in the rafted structure, dislocations can move by glide or climb through the γ channels, which is a process which requires lower stress and thus results in poorer mechanical performance.

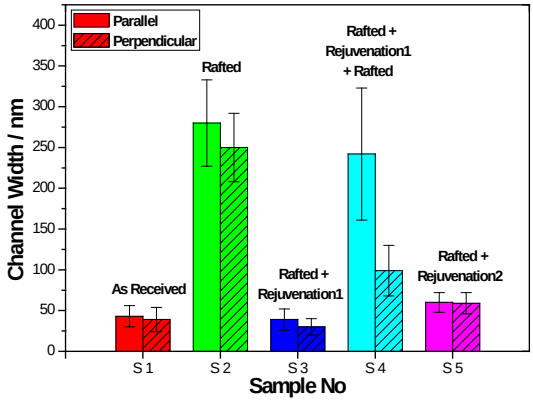

Figure 8: γ channel width measurements between the secondary' particles of head sections for the five different heat treated samples measured in parallel and perpendicular directions.

Although the average parallel γ channel width of S2 (280 nm) and S4 (242 nm) show no significant difference, the channel widths in the perpendicular direction are substantially different. S2 has an average width of 250 nm in the perpendicular direction, whilst S4 was only 99 nm. The difference in channel width indicates that the degrees of rafting are different in these samples. In order to define the degree of rafting, a rafting parameter R was used. For a cuboidal γ′ particle a rafting parameter of 0.5 would be expected. As shown in Table 5, the rafting parameter of S1, S3 and S5 is very small, around 0.5, because the L and T values are the same. However, for rafted samples, rafting results in a very large L but small T value, which leads to a greater R value. The R value for S4 is much larger than S2, which confirms the observation that S4 has a more continuous rafted microstructure. With these continuous broader channels, dislocations can move more easily through the structure, which consequently leads to a reduction in tensile strength.

The microstructure of the rejuvenation 1 sample (S3) showed the same γ′ size, morphology and distribution as the as-received sample (S1), as well as degree of rafting, which was consistent with the tensile test results. These microstructures indicate that the rejuvenation procedure for S3 used here restores the microstructure of a previously rafted sample to a microstructure which is apparently equivalent to that of the as-received structure. However, when the rejuvenation 1 (S3) sample experienced a subsequent further rafting treatment (S4), the microstructure showed a greater extent of rafting than the sample which had received only one rafting treatment, sample S2. It is possible that any chemical segregation present within the alloy has not been removed during rejuvenation, which was then enhanced by the second rafting treatment with an accompanying reduction in mechanical properties. This could explain why, on the microstructural level, the as-received (S1) and rejuvenated (S3) sample are very similar but they showed a very

different mechanical performance and microstructure after undergoing a subsequent “return to service” degradation treatment.

Chemical Segregation Analysis of Dendrite Core and Interdendritc Region

According to [14-16], the degradation not only degrades the microstructure but also causes chemical segregation, which later affects the mechanical performance. As previously shown, the rejuvenation heat treatment appears to have recovered most of the microstructure to the as-received conditions, but it is important to examine the chemical segregation level of these samples after rejuvenation. Since directional coarsening of the γ' is a diffusive process, which is very dependent on the movement of the alloying elements, the chemical segregation and homogeneity have been carefully measured with respect to the dendrite structure. Figure 9 shows optical microscope images of these samples showing dendrite cores and interdendritic regions with accompanying EDS area analysis results in Fig. 10.

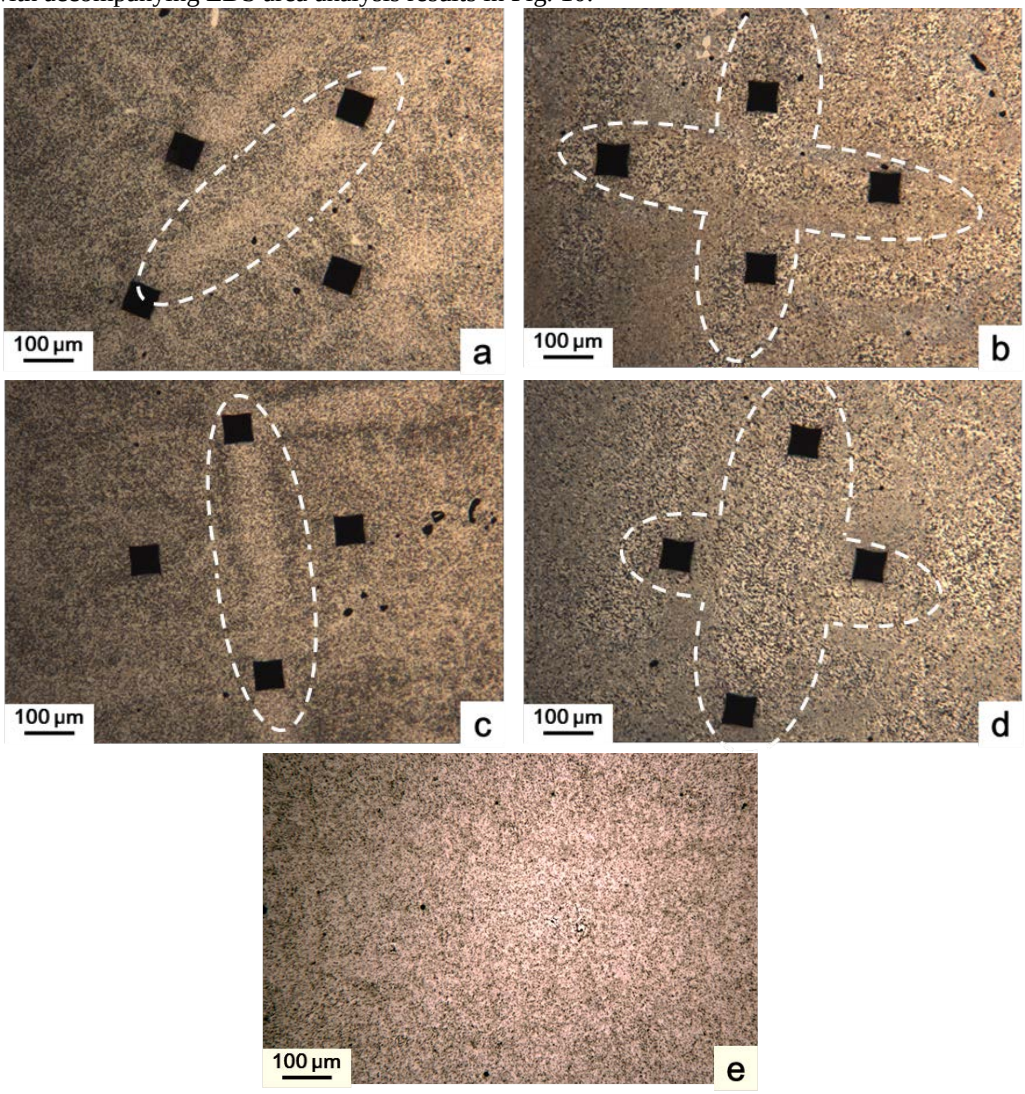

Figure 9: Optical microscopy images showing dendrite structures in; a) S1, as-received, b) S2, rafted, c) S3, rafted + rejuvenation 1, and d) S4, rafted + rejuvenation 1+ rafted, e) S5, rafted + rejuvenation 2.

In Fig. 9, the dendritic structures of S1-S4 are very clear and the structures increase in size after the rafting treatment. After rejuvenation 2 (S5), no dendritic structure was observed, which may indicate that a more homogeneous composition and microstructure were obtained. The chemical composition difference results are shown in Fig. 10, where this defined as the difference in chemistry between the IDR and the DC. Most of the elements show clear chemical segregation differences. Therefore, since the behaviour of Al, Ti, Ta, W and Re were most obvious, the chemical segregation difference of these elements was used to represent the chemical difference trend in this study. It has been found that Al, Ti and Ta are rich in the IDR, but consistently lower in DC, whilst Re and W exhibit contrary trends, which is in good agreement with Karunaratne *et al*. [17]. According to the chemical segregation results, the sequence of the chemical segregation from large to small is S4, S2, S3 and S1. The chemical segregation in the as-received sample is the smallest. It is clearly shown that chemical segregation has increased when the sample has undergone a rafting treatment. Although, rejuvenation 1 has recovered some segregation e.g. Ti and Ta, it has not recovered to the as-received condition, but is closer to the rafted conditions. This residual segregation is due to the slower diffusing elements such as Re and W. According to Karunaratne *et al*. [17], the interdiffusion coefficients of Re and W at the rejuvenation temperature are the slowest, which means chemical segregations of these elements are very difficult to eliminate with short term rejuvenation or homogenisation [6, 15-17]. When the rejuvenation 1 sample (S3) experiences a further degradation treatment, the chemical segregation increases even more. Chemical segregation is the key explanation for the reduction in the performance after the second rafting heat treatment (S4), as the segregation of slowly diffusing elements such as Re and W, is not fully removed during the short time rejuvenation.

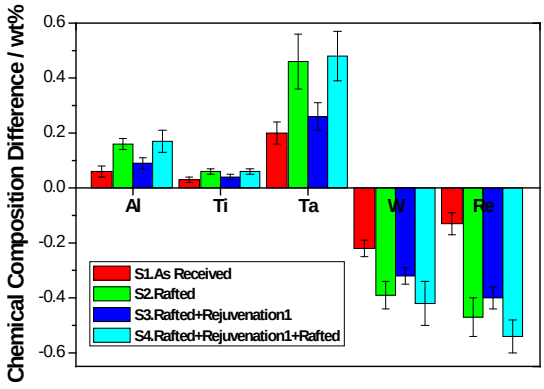

Figure 10: Chemical composition difference between dendrite core and interdendritic regions

In order to determine whether the length of rejuvenation could eliminate these detrimental segregation effects, a more extended rejuvenation procedure, rejuvenation 2, was applied to the rafted sample. On a microstructural level (Fig. 5), the size and distribution of cuboidal γ′ is equivalent to the size of as-received (S1) and rejuvenation 1 (S3). Very fine tertiary γ′ with a size around 30 nm was also found. This microstructure is same as rejuvenation 1(S3). However, the rejuvenation 2 sample (S5) shows no a clear dendrite structure, which indicates a more homogeneous structure may be obtained in this sample. Therefore, in order to make a comparison of chemical segregation in this sample, 20 EDS area analysis boxes with a size of 20x20 μm were randomly carried on as-received, rejuvenation 1 and rejuvenation 2, by using the difference between the maximum and minimum chemical composition to present the inhomogeneity of the samples, as shown in Fig. 11. It has been found that the chemical inhomogeneity is smallest in the as-received sample. For the rejuvenation 1 sample, there exists

a large degree of chemical inhomogeneity which is much greater than as-received conditions, especially for heavy elements, such as W and Re. Encouragingly, rejuvenation 2 (S5) has reduced the inhomogeneity, to levels very close to the as-received condition. The microstructure and chemical homogeneity results are very positive for rejuvenation 2, indicating that an extended heat treatment is required for full rejuvenation.

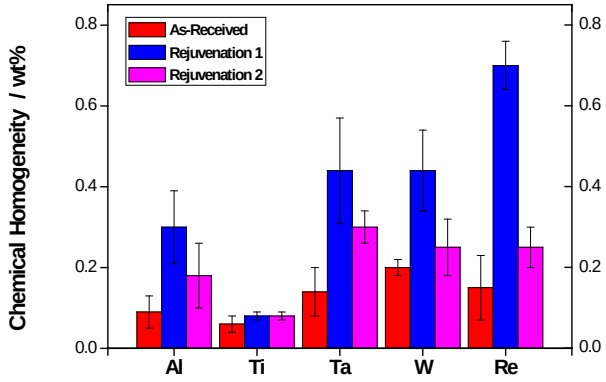

Figure 11: Chemical homogeneity of as-received, rejuvenation 1 and rejuvenation 2 based on 20 randomly selected EDS area analyses.

CONCLUSIONS

The microstructural evolution and tensile behaviour of differently degraded and rejuvenated CMSX-4 samples have been examined. A few conclusions can be drawn as follows:

1. The resulting tensile properties, developed in CMSX-4 in its various states of degradation and rejuvenation, resulted from changes in the area fraction of secondary γ′ particles, γ channel width and the precipitation of the tertiary γ′ in the channels.
2. Although the microstructure of the rejuvenation 1(S3) and as-received (S1) samples are very similar to each other, their performance was distinct differently after they had undergone another high temperature degradation, resulting a large difference in channel width, degree of rafting and mechanical behavior.
3. Chemical segregation is the key explanation for the reduction in the performance after the second rafting heat treatment, as the segregation was not removed from the rejuvenation 1 and then was enhanced by second degradation process.
4. An extended rejuvenation heat treatment has significantly reduced the chemical segregation difference and inhomogeneity within the alloy, with the same distribution, size of secondary γ′ and tertiary γ′ inside channels. This result suggests that the mechanical performance will be improved relative to the shorter rejuvenation heat treatment. The mechanical test results are currently underway.

ACKNOWLEDGEMENTS

The authors would like to acknowledge the support of the Technology Strategy Board (Project Number TP/5/MAT/6/I/H0101B) and the following companies: Alstom Power Ltd., E.ON New Build & Technology Limited, Doosan Babcock, National Physical Laboratory and QinetiQ for their valuable contributions to the project.

REFERENCES

[1] Reed, Roger C, The Superalloys: fundamentals and applications. Cambridge University Press, (Cambridge, 2006), pp. 11-23

[2] Lvova, E., and D. Norsworthy. "Influence of Service-induced Microstructural Changes on the Aging Kinetics of Rejuvenated Ni-based Superalloy Gas Turbine Blades." J. Mater. Eng. Perform, Vol.10, No. 3 (2001), pp. 299-312.
[3] Baldan, A., "Rejuvenation Procedures to Recover Creep Properties of Nickel-base Superalloys by Heat Treatment and Hot Isostatic Pressing Techniques." J. Mater. Sci. Vol.26, No. 13 (1991), pp. 3409-3421.
[4] James, A., "Review of Rejuvenation Process for Nickel base Superalloys." Mater. Sci. Technol., Vol.17, No.5 (2001), pp. 481-486.
[5] Matan, N., et al. "On the Kinetics of Rafting in CMSX-4 Superalloy Single Crystals." Acta Mater., Vol.47, No.7 (1999), pp. 2031-2045.
[6] Reed, R. C., et al. "Kinetics of Rafting in a Single Crystal Superalloy: Effects of Residual Microsegregation." Mater. Sci. Technol., Vol.29, No.7 (2013), pp. 775-780.
[7] ASTM Standard E8/E8M-08, "Standard Test Methods for Tension Testing of Metallic Materials." ASTM international, West Conshohocken, PA, 2008.
[8] Yao, Z., et al. "Effect of Rejuvenation Heat Treatments on Gamma Prime Distributions in a Ni based Superalloy for Power Plant Applications." Mater. Sci. Technol., Vol.23, No.8 (2013), pp. 893-902.
[9] Ignat, M., "Microstructures Induced by a Stress Gradient in a Nickel-based Superalloy." Acta Metall., Vol.41, No.3 (1993), pp. 855-862.
[10] Koul, A. K., and R. Thamburaj. "Serrated Grain Boundary Formation Potential of Ni-based Superalloys and Its Implications." Metall. Trans. A, Vol.16, No.1 (1985), pp. 17-26.
[11] Durand-Charre, M., The Microstructure of Superalloys. Gordon& Breach , (Amsterdam, 1997), pp. 69-75.
[12] Sengupta, A., et al. "Tensile Behavior of a New Single-crystal Nickel-based Superalloy (CMSX-4) at Room and Elevated Temperatures." J. Mater. Eng. Perform., Vol.3, No.1, (1994), pp. 73-81..
[13] Liu, L. R., et al. "Microstructural Evolution of a Single Crystal Nickel-base Superalloy During Thermal Exposure." Mater. Lett., Vol.57,No.29, (2003), pp. 4540-4546..
[14] MacKay, R. A., and M. V. Nathal. "γ′ Coarsening in High Volume Fraction Nickel-base Alloys." Acta Metall. Vol.38, No.6, (1990), pp. 993-1005.
[15] Cheng, K. Y., et al. "Influence of Local Chemical Segregation on the γ′ Directional Coarsening Behavior in Single CrystalSsuperalloy CMSX-4." Mater. Charact. Vol.60, No.3, (2009), pp. 210-218.
[16] Epishin, A. I., et al. "Residual Stresses in the Dendritic Structure of Single-crystal Nickel-based Superalloys." Physics of Metals and Metallography, Vol.100, No.2, (2005), pp. 192-199.
[17] Karunaratne, M. S. A., et al. "Modelling of the Microsegregation in CMSX-4 Superalloy and Its Homogenisation during Heat Treatment." *Superalloys 2000 Conf*, Champion, Pennsylvania, Septermber 21, 2000. PP. 263-272.